Part I

Modelling Dislocation Properties and Behavior

DISLOCATIONS AND PLASTICITY IN SILICON CRYSTALS BY 3-D MESOSCOPIC SIMULATIONS

L.P. KUBIN *, A. MOULIN * and P. PIROUZ **
* LEM, CNRS-ONERA, 92322 F-Châtillon Cedex, kubin@onera.fr, amoulin@zig.onera.fr
** Dept. MSE, CWRU, Cleveland, OH 44106-7204, USA, pirouz@cwmsd.mse.cwru.edu

ABSTRACT

Several problems related to the dynamics of dislocation sources and the plasticity of silicon crystals are investigated with the help of a mesoscopic simulation. The questions successively examined are the dynamics of a source of perfect dislocations and the conditions under which perfect or partial dislocations are emitted by a source. This leads to a discussion of the initial steps of the model proposed by Pirouz for mechanical twinning and, further, to the suggestion that a relation may exist between several transitions experimentally observed at low temperatures in elemental or compound semi-conductors: a change in the slope of the yield stress vs. temperature curves, a brittle-to-ductile transition and a change in the nature of the mobile dislocations. Finally, simulations are presented of the yield point phenomenon that is a well-known feature of Si and Ge crystals. The results are discussed in terms of evolutionary laws for the total dislocation density during straining.

INTRODUCTION

Silicon is the model material where dislocation velocity is the best characterized and for which a large amount of experimental data exists in the literature (see e.g. [1] for a review). Dislocation glide in the diamond cubic (dc) structure occurs by the breaking and reconstruction of covalent bonds, which leads to the occurrence of high Peierls forces. Hence, in a large range of temperatures (typically below about 1200 K), the energy involved in the movement of a dislocation from one Peierls valley to the next is larger than the self-energy of the dislocation. As a consequence, the dislocation loops tend to be straight, often forming hexagonal loops with the sides of the hexagon parallel to the three <110> close-packed directions of a {111} slip plane. Dislocation motion then occurs by the formation of kink pairs over the primary Peierls valleys and the migration of the kinks over the secondary Peierls valleys. These processes are usually modeled within the frame of the diffusing kink model [2].

However, to understand plastic flow it is also necessary to model other processes which are less easy to approach experimentally, for instance the mechanisms of dislocation multiplication. In this context, the recent development of fully three-dimensional mesoscopic simulations of dislocation dynamics allows to check the basic assumptions of several existing models. The present paper is thus concerned with several applications of such mesoscopic simulations to the case of silicon crystals.

The main principles of this simulation are first presented. Two types of applications are then discussed. One is concerned with the dynamics of a single Frank-Read source, with a source segment that is either a perfect dislocation or a dislocation dissociated into two Shockley partials. In the latter case, it is shown that the source may in certain conditions emit a partial dislocation, as has been predicted by Pirouz [3]. The existence of a transition between the emission of partial versus perfect dislocations may have several possible consquences on the mechanical properties that are discussed with respect to the available experimental data. Finally, such simulations can also be a powerful tool for the understanding of particular features of the stress-strain curves, as examplified by a study of the yield point phenomenon in relation to the multiplication mechanisms.

MESOSCOPIC SIMULATIONS

Method

The simulation code used in the present work derives from an existing mesoscopic simulation dedicated to the simulation of dislocation dynamics in FCC crystals [4]. By "mesoscopic" is meant

Mat. Res. Soc. Symp. Proc. Vol. 538 © 1999 Materials Research Society

here that dislocations are treated as linear discontinuities in an elastic isotropic continuum. Space is discretized, the smallest distance considered in the continuum being the critical annihilation distance of edge dipoles, $y_e \sim 6b$, where b is the magnitude of Burgers vector of the perfect dislocations [5]. This distance marks the border-line between the domain of dislocation core properties and the domain of elastic interactions, the former being accounted for by phenomenological local rules. As a consequence, the simulation is based on a discrete fcc lattice, mimicking the diamond cubic lattice in the present case, whose parameter is 2.71 nm. The resolved shear stress applied on each dislocation segment includes the applied stress, the line-tension stress and the interaction stress corresponding to long range elastic interactions. More detail about the discretization of the dislocation lines and the implementation of the dynamics and of the local rules can be found in [6, 7].

The modifications introduced were intended to account for the main consequences of the high Peierls forces at the mesoscopic scale, viz. the hexagonal shapes of the gliding dislocation loops and the particular stress vs. velocity laws associated with the kink pair mechanism. As discussed in [8], this involves the discretization of the segment orientations into three elementary characters, screw and mixed ± 60°, in place of the initial edge/screw description. In addition, a stress and temperature-dependent velocity rule was introduced for each segment. Within the kink diffusion model of Hirth and Lothe [2], the prefactor of the thermally activated velocity depends on whether the length L of the considered segment is smaller or larger than a temperature-dependent critical length L_c. The two corresponding expressions are reproduced here without demonstration.

For $L < L_c$, only one kink pair propagates at any time along the dislocation line and the mean free path of the kink pair is L. The velocity of the dislocation segment is then given by:

$$v = L\frac{\tau^* bh^2}{kT}\upsilon_D \exp\left(-\frac{2E_{kf}+E_{km}}{kT}\right)\exp\left(\frac{2S}{k}\right), \quad (1)$$

where h is kink height, ν_d is the Debye frequency, k the Boltzmann constant, τ^* the resolved shear stress, and T the absolute temperature. E_{kf} and E_{km} denote respectively the formation and migration energies of a single kink. S is a correcting entropy term introduced by Marklund [9]. In this regime, which corresponds to large stresses and low temperatures, the velocity of a segment is proportional to its length.

For $L > Lc$, the mean free path of kinks is smaller than the segment length. The stress velocity law is then of the form:

$$v = \frac{2a_o\tau^* bh^2}{kT}\nu_D \exp\left(-\frac{E_{kf}+E_{km}}{kT}\right)\exp\left(\frac{S}{k}\right), \quad (2)$$

where a_o is the lattice parameter. This law applies at high temperatures and low stresses and has been the object of numerous experimental checks [1, 10]. In this regime, the velocity law can be rewritten in the form

$$v = \frac{dx}{dt} = \alpha\tau^* f(T) \quad (3)$$

where x denotes the position of the segment, f(T) includes the temperature dependence and α is a constant. Hence, a change of temperature is strictly equivalent to a change of time scale. Considering for instance the configuration of dislocation loops emitted by a Frank-Read (FR) source, a temperature change modifies the dynamics but not the geometry. The transition between the two velocity regimes of eqs. 1 and 2 has been experimentally observed by Louchet [11] and Hirsch et al. [12].

Validation

Two algorithmic parameters govern the dynamics [8]. One is the elementary time step dt; this parameter determines the frequency of the resolved stress computations, of the dislocation

displacements and of the treatment of particular events such as dislocation annihilation, dislocations running out from the free surfaces of the simulated crystal, cross-slip, etc. The other parameter is a discretization parameter, L_d, governing the creation of new dislocation segments at the pinning points of dislocation sources. Thanks to this rather simple set of rules, the present simulation can reproduce the complete operation of a FR source from a segment pinned at its two ends (cf. fig. 1).

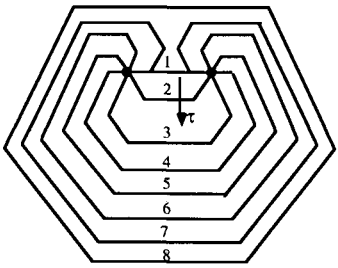

Fig.1. Successive configurations of a dislocation loop emitted by a Frank-Read source in a (111) slip plane (T = 1000 K, τ = 35 MPa, L = 0.81 μm).

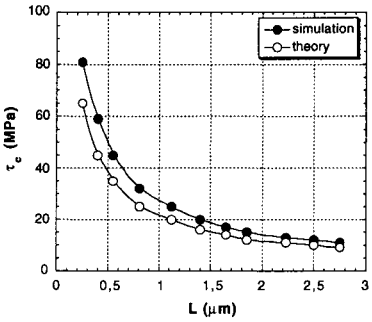

Fig. 2. Critical stress τ_c as a function of source length L (T = 1000 K). The theoretical values refer to circular loops [13].

The two parameters dt and L_d may induce artefacts if their values are not correctly defined. For instance, the time step dt must be kept small enough to ensure the convergence of the equations of motion of individal dislocation segments. It has also to be optimized in order to reduce the computation time, which is the main limitation of the simulation when large dislocation densities are involved. The optimal ranges for these parameters were defined by considering the critical bowing-out stress of an initially pinned segment, τ_c, which is defined as the lower applied stress for which a dislocation loop can be formed. τ_c is a static and temperature-independent quantity, which stems from a static equilibrium between the line tension stress and the applied stress. Fig. 2 shows the variations of τ_c versus the source length at T = 1000 K. The computed values are 20% larger than the ones predicted by Foreman [13] for circular loops, which is due to the fact that we are dealing here with hexagonal loops of larger self-energy.

By checking the stability of the critical stress values with respect to changes of the two parameters, one can define optimum values for these parameters for each simulation condition, as defined by the temperature, the applied stress and the initial source length. As a consequence, all the results presented in what follows are independent of the algorithmic construction of the simulation. It is worth noting that the time steps used in the case of silicon (typically dt = 5×10^{-2} s) are much larger than those used for fcc crystals (typically 10^{-9} s or less). This is due to the low dislocation mobilities induced by the lattice friction.

STUDY OF A SINGLE DISLOCATION SOURCE

The interest of such a simulation is that, in contrast to the available models, it does not make any phenomenological assumption regarding the conditions for dislocation emission by the source. From an investigation of the dynamics of a FR source as a function of stress and temperature, it appears that the critical parameters are the size of the innermost loop and the time it takes to form it (i.e., to reach step 8 of fig. 1). Fig. 3 shows the evolution of the (equivalent) radius of this loop as a function of temperature under a constant applied stress 1.3 times larger than the critical stress and for an initial length of the source segment of 0.8 μm. The double plateau obtained in fig. 3 directly

illustrates the influence of the two velocity regimes for the dislocations. According to the theoretical value of the critical transition length L_c, all the segments are in the length-independent regime part of the velocity law (eq. 2) above T = 1000 K. In this domain, which corresponds to the high temperature plateau in fig. 3, a change in temperature can be accommodated by a change in the time scale of the source emission (eq. 3) without any modification in the geometry of the emitted loop. For T < 800 K, all the segments are in the length-dependent regime of the velocity law, which corresponds to the low temperature plateau of fig. 3. Considering the velocities of a given segment in this low temperature regime and at two different temperatures, $v = \alpha f(T) L\tau^*$ and $v' = \alpha f(T') L\tau^*$, we notice that the ratio $v/v' = f(T)/f(T')$ is length-independent and only depends on temperature. Then, for the same reason as before, the emitted configurations follow a simple scaling law in this domain. Between 800 K and 1000 K a mixed regime is obtained, the small segments being in the length-dependent regime and the long ones in the length-independent one. Since in real crystals one should always have a rather wide distribution of segments lengths, this first result indicates that the combination of the simple rules involved in the emission of a FR source may lead to rather complex effects.

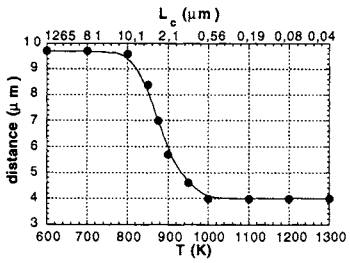

Fig. 3. Radius of the first complete loop vs. temperature (τ = 35 MPa, L = 0.81 μm).

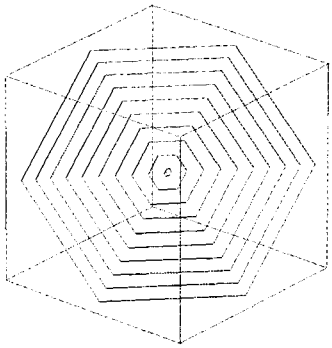

Fig.4. Typical configuration of dislocation loops emitted by a source (same conditions as fig. 1). The crystal size is 550 μm.

In a next step the concentric loops emitted by a single source (cf. fig. 4) are considered. These configurations seem to present a uniform spacing between the successive loops, in agreement with an assumption commonly made in the modeling of source emission. However, closer examination reveals that the spacings can deviate from average by about 10%, the deviations being governed by the evolution of the backstress on the source segment [14,15]. A quantitative study was performed of the effective stresses acting on the innermost dislocation loop in its glide plane and in its cross-slip plane, respectively τ_G^* and τ_{CS}^*. The ratio τ_{CS}^*/τ_G^* is found to increase with the number of emitted loops. This is illustrated by fig. 5 where it is plotted for several values of (stress, temperature) pairs corresponding to the upper yield point of silicon. These values were computed in the steady state or saturation regime, where a new loop is formed by the source every time a loop disappears at the free surface of the simulated crystal. As the ratio τ_{CS}^*/τ_G^* increases monotonically with temperature, the occurrence of cross-slip events is favoured in a purely mechanical way.

To illustrate the complex combination of phenomena involved in the source emission, fig. 6 shows a plot of the dislocation density produced in a slip plane by a single source operating in steady state conditions, as a function of applied stress and temperature. The (stress, temperature) pairs shown in fig. 5 are reported on this plot. The interesting fact is that points 1 and 5 correspond to the same saturation density, while according to fig. 5 the cross-slip probability should be quite different. In fact, point 1 corresponds to high stress/low temperature conditions, where the dislocation density is essentially driven by the length-dependent regime of the velocity law. Due to the high applied stress, the interaction stresses represent a small relative fraction of the

effective stress and they cannot influence cross-slip. In contrast, point 5 corresponds to low stress/high temperature conditions, where the dislocation density is limited by the low applied stress. In this case, the elastic interactions between dislocations are significant compared to the applied stress, and this leads to high values of the ratio τ_{CS}^*/τ_G^*. Hence, configurations 1 and 5 are very similar from a geometrical point of view but are intrinsically governed by quite different mechanisms.

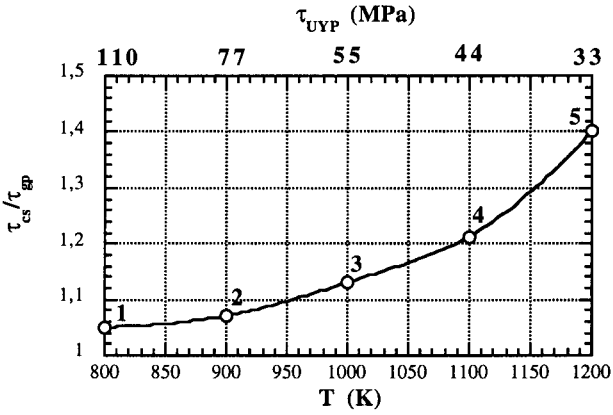

Fig. 5. Simulated values of the ratio τ_{CS}/τ_G for couples of stress and temperature values corresponding to the upper yield stress of silicon.

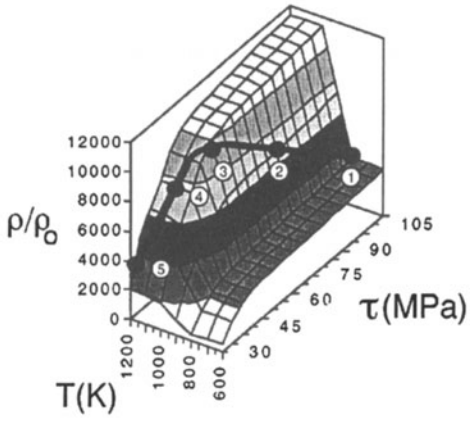

Fig. 6. Saturation density (scaled by the initial density ρ_o) in the glide plane of a source as a function of temperature and applied stress. The source length is 0.81 μm and the 2-D crystal size is 550 μm.

This study can easily be extended to the case where the dislocation mobilities depend on the character of the moving dislocation, provided that the anisotropy of dislocation mobility is known

theoretically or experimentally. As an illustration, fig. 7 shows the changes in source configuration obtained in the case where screw and 60° dislocations have different mobilities (the values are those quoted in [1] for germanium and their ratio is denoted by g) and in the case where dislocation segments of opposite sign have different mobilities (the values are typical ones quoted in [1] for III-V compounds).

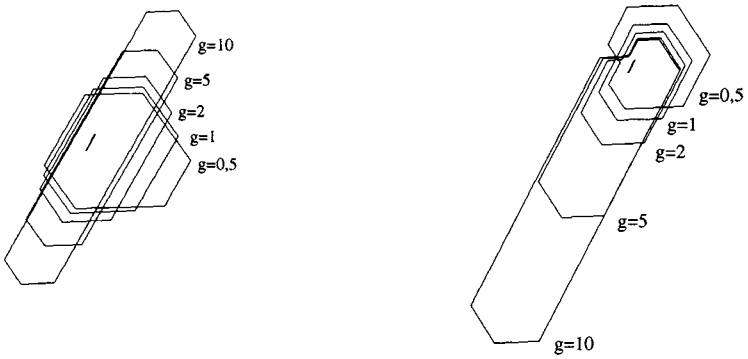

Fig. 7. Influence of the velocity anisotropy ratio g on the geometry of the first formed loop (same conditions as in fig. 1).- (a) between screw and 60° dislocations (case of Ge, $g = v_{60°} / v_{screw}$). - (b) between α and screw, or α and β dislocations (case of III-V compounds, $g = v_{\alpha} / v_{screw, \beta}$).

SOURCES WITH DISSOCIATED DISLOCATIONS

Perfect and Partial Frank-Read Sources

Up to now we have considered only perfect dislocations. The dynamics of dislocation sources made up of dislocations dissociated into two Shockley partial dislocations was investigated with the aim of identifying the particular conditions under which partial dislocations can be emitted [16]. For this purpose, two new features were introduced in the simulation. If γ is the stacking fault energy (γ = 69 mJ/m^{-2} in silicon) and $b_p = |\mathbf{b}_p| = |1/6\langle 112\rangle|$ is the modulus of the Burgers vector of the Shockley dislocations, the stacking fault induces a drag stress $-\gamma/b_p$ on the leading partial and $+\gamma/b_p$ on the trailing partial. The velocities of the Shockley partials were expressed by the same functional forms as those used for perfect dislocations, as justified by Yasutake et al. [17]. In addition, the dependence of the velocities on dislocation character was introduced. Due to the lack of experimental data on this subject, this velocity anisotropy of the partials was assumed to be temperature-independent and the values adopted were those determined by Wessel and Alexander at 800 K [18]. Although no experimental measurement is available to date, it is well established, however, that this anisotropy increases with decreasing temperature [19].

The initial configuration of a dissociated source segment is shown in fig. 8(a). To characterize the type of dislocation emitted by the source, two quantities are of interest which are defined in fig. 8(b). At the moment that the first loop (made up by the leading partial) closes up, the distance d_1 measures the equivalent of a dissociation width, and d_2 measures the advance of the trailing partial with respect to the initial leading segment. By convention, a partial dislocation is considered as being emitted when a faulted loop is formed ($d_1 >> d_2$) with $d_2 < 200$ nm.

A factor that strongly influences the behavior of the partial dislocations is what might be called the "Escaig effect". For a fixed orientation of the applied stress, the resolved stresses on the Shockley partials are not identical and tend to either constrict or expand the stacking fault ribbon.

The latter case is met with a [100] stress orientation which is the one used here. For straight infinite dislocations, a simplified calculation due to Alexander and Wessel [18] estimates a critical stress of 300 MPa for an infinite extension of the stacking fault ribbon. Under a stress value fixed at 350 MPa in a first step, a clear transition in source emission is observed. This is illustrated in fig. 9 which shows the variations of the two geometrical parameters d_1 and d_2 within a wide range of temperature. Two characteristic source configurations are shown in addition. As expected, perfect dislocations are emitted at high temperatures (1100K), whereas source emission at 800K leads to the formation of a faulted loop. This transition can be interpreted in terms of the coexistence of the two velocity regimes (eqs. 1 and 2) and of their influence on the dynamics of source emission [16].

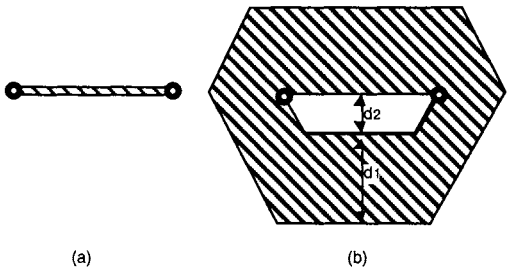

Fig. 8. Initial source configuration (a) and configuration obtained after the formation of the first loop (b). The striped area represents the faulted region.

Consequences

It must be noticed that once a faulted loop has been formed, the source shuts off and cannot re-emit a second partial dislocation. Indeed, this would involve the dissociation of the source dislocation within a faulted plane, thus producing a "forbidden" stacking fault of high energy. This locked configuration actually constitutes the first step of the model proposed by Pirouz [3, 19] for mechanical twinning in semiconductors. Further steps of this model involve the recombination and cross-slip of the source segment, where the order of the partials has been exchanged, and the production of faulted loops in successive slip planes.

A systematic investigation of the transition between perfect and partial emission by dislocation sources was performed as a function of stress and temperature. The results are summarized in fig. 10. This figure shows the values of d_2, the distance between the trailing and leading partials once the first loop has closed up, as a function of stress and temperature. Using the criterion mentioned above to define partial emission, the latter occurs in the domain shown in white in fig. 10. Although this estimate is based on several assumptions and is carried out with a favourable orientation of the applied stress, it shows that the first step of Pirouz model is likely to occur at low temperatures and under rather high stresses.

To fix the ideas, the computed critical stress at 950 K is about 400 MPa, a value much larger than the yield stress of silicon at such a temperature. In silicon, the Brittle to Ductile Transition (BDT) occurs at about 850 K (in non-predeformed crystals, this value is sensitive to the applied strain rate), under stresses typically of the order of a few tens of MPa. Thus, very high stress concentrations are needed to obtain partial emission, and possibly mechanical twinning, in the ductile regime. If, however, one considers compression tests on predeformed specimens and/or under a superimposed hydrostatic pressure, or indentation tests, stress levels can be reached that are typically those predicted by fig. 10 (see e.g. [20, 21]). Hence, the qualitative estimate provided by the simulation indicates that mechanical twinning, or at least its first step according to the model of Pirouz, is more likely to occur below the BDT than above. For the sake of completeness, it must be mentioned that the partial dislocations of a twin can also be nucleated at a surface heterogeneity [19, 22, 23], a situation that cannot be investigated with the present simulation.

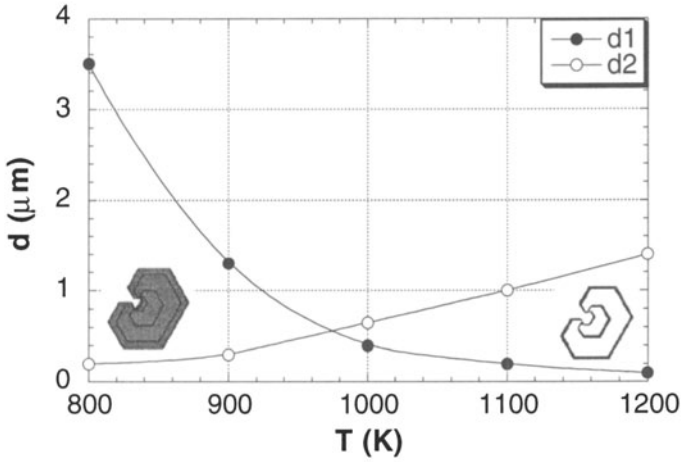

Fig. 9. Temperature dependence of the two coefficients d_1 and d_2 characterizing the source geometry vs. temperature (applied stress: 350 MPa). Typical simulated configurations of perfect and dissociated sources, for large and small values of d_2 respectively, are inset.

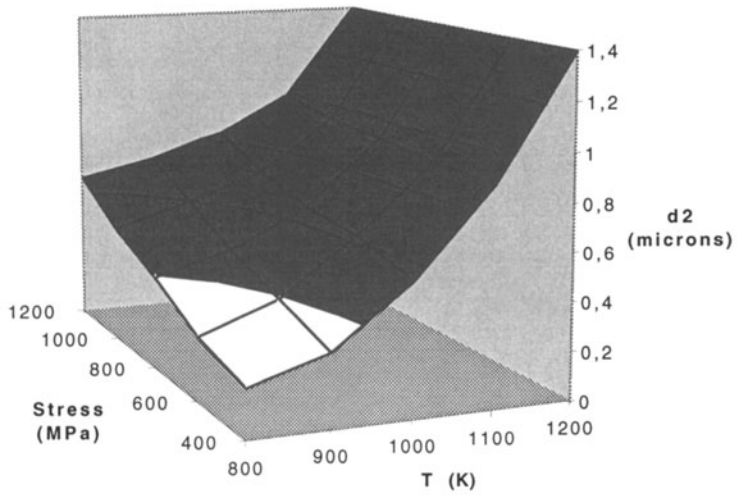

Fig. 10. Temperature and stress dependence of the geometrical parameter d_2. The source is considered as having emitted a partial dislocation when $d_2 < 200$ nm. A partial dislocation is emitted in the domain shown in white and perfect dislocations in the domain shown in black.

The fact that the transition in the mode of operation of a dislocation source occurs approximatively in the same temperature range as the BDT suggests that the two may be related. This possibility has been investigated by Pirouz et al. [24] who suggested a new model correlating